Applied Surface Science 258 (2012) 4417–4423

Contents lists available at SciVerse ScienceDirect

Applied Surface Science

journal homepage: www.elsevier.com/locate/apsusc

Influence of sodium bis(2-ethylhexyl) sulfosuccinate (AOT) on zinc electrodeposition

I.L. Lehr, S.B. Saidman*

Instituto de Ingeniería Electroquímica y Corrosión (INIEC), Departamento de Ingeniería Química, Universidad Nacional del Sur, Av. Alem 1253, 8000 Bahía Blanca, Argentina

ARTICLE INFO

Article history:
Received 27 July 2011
Received in revised form
21 December 2011
Accepted 30 December 2011
Available online 5 January 2012

Keywords:
Zinc
Electrodeposition
Stainless steel
AOT

ABSTRACT

This work is a study of the electrodeposition of zinc onto SAE 4140 steel electrodes using solutions containing zinc sulfate and bis(2-ethylhexyl) sodium sulfosuccinate (AOT). The influence of different parameters such as electrolyte concentration, electrodeposition time and temperature on the morphology of the electrodeposits was analyzed. The deposits were characterized by scanning electron microscopy (SEM), energy dispersive X-ray (EDX) and X-ray diffraction. The variation of open circuit potential over time in chloride solutions was also evaluated. The nucleation-growth process and consequently the morphology of the electrodeposits are modified in the presence of AOT. The surfactant induces the formation of a porous deposit.

1. Introduction

Surfactants are commonly used in various fields of electrochemistry such as electroplating, corrosion protection, batteries and fuel cells, electrocatalysis among others [1]. The specific activity of the surfactants depends on their concentration and it is often associated with adsorption of molecules on the surface of the cathode during electrodeposition. When the concentration is near the critical micelle concentration (cmc) formation of bilayers or multilayers at the interface of the electrode occurs [2]. The adsorption of surfactant aggregates on electrodes can have great effects on the kinetics of electron transfer and consequently on the electroplating process.

Zinc and zinc alloys are the most used sacrificial coatings for protecting ferrous materials against corrosion in diverse technological fields. Zinc-rich paints are also very effective to avoid corrosion. A lot of studies deal with the electrodeposition of zinc and zinc alloys and the deposits were obtained under different operating conditions depending on the application. Surfactants are usually added to the solution for deposition in order to improve the efficiency of the process and the characteristics of the deposits. As part of the continuous effort in improving the corrosion resistance of iron and its alloys, it was also demonstrated more recently that the incorporation of zinc particles uniformly distributed inside a conducting polymer or a sol–gel film improves the corrosion protection properties of the coatings [3–5].

On the other hand, fabrication of metallic micro and nanostructured Zn deposits is an actively researched topic [6–9].

Sodium bis(2-ethylhexyl)sulfosuccinate, also known as AOT, is an anionic surfactant widely used in the formation of reverse micelles. The molecule has two bulky alkyl tails and a small negative charged SO_3^- headgroup. Previous works have shown that an AOT-containing solution can be used for the electropolymerization of pyrrol onto Al [10], Fe [11] and Ti [12]. The presence of surfactant allows the electrosynthesis of stable, adherents and homogeneous films with good anticorrosive properties. Moreover, the incorporation of a large and immobile anion like AOT conditions the ion-exchange behavior of the polymer matrix. The AOT molecule plays the dual role of dopant and surfactant.

The present study aims to contribute to the knowledge of Zn deposition in the presence of surfactants. The objective was to evaluate the influence of AOT on the electrodeposition process and on the morphology of deposits. To the best of our knowledge this system is studied for the first time. The electrodeposition process was characterized by cyclic voltammetry, current–time transients, SEM-EDX analysis and X-ray diffraction.

2. Experimental

Electrodes were prepared from SAE 4140 steel rod samples. The rods were embedded in a Teflon holder with an exposed area of 0.070 cm^2. Before each experiment, the exposed surfaces were polished to a 1000 grit finish using SiC, then degreased with acetone and washed twice with distilled water. Following this pretreatment, the electrode was immediately transferred to the

* Corresponding author. Tel.: +54 291 4595182; fax: +54 291 4595182.
E-mail address: ssaidman@criba.edu.ar (S.B. Saidman).

0169-4332/$ – see front matter © 2012 Elsevier B.V. All rights reserved.
doi:10.1016/j.apsusc.2011.12.127

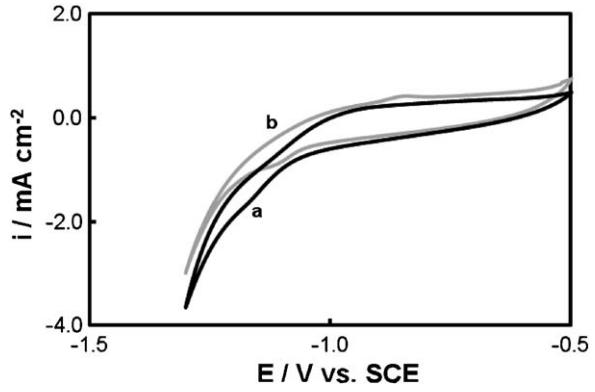

Fig. 1. Cyclic voltammograms for SAE 4140 steel electrode at 0.01 V s^{-1} in: (a) 0.05 M Na_2SO_4; (b) 0.05 M AOT + 0.05 M Na_2SO_4. Initial potential: −0.5 V. The first cycle is displayed. The temperature was 20 °C.

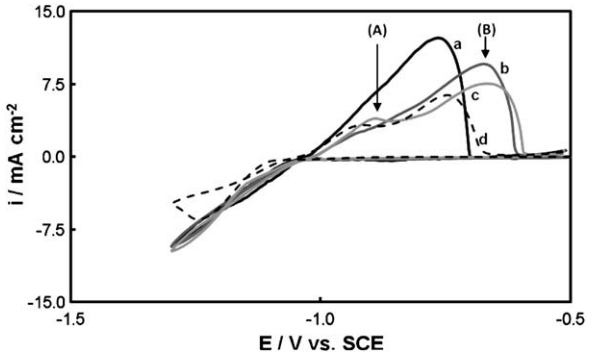

Fig. 2. Cyclic voltammograms for SAE 4140 steel electrode at 0.01 V s^{-1} in 0.05 M $ZnSO_4$ + *x* M AOT, pH 6.3 solution with: (a) *x* = 0, (b) *x* = 0.005, (c) *x* = 0.01 and (d) *x* = 0.05. Initial potential: −0.50 V. The first cycle is displayed. The temperature was 20 °C.

electrochemical cell. All the potentials were measured against a saturated calomel electrode (SCE) and a platinum sheet was used as a counter electrode.

Electrochemical measurements (cyclic voltammetry, potentiostatic polarization, open circuit potential) were done using a potentiostat–galvanostat PAR Model 273A. A dual stage ISI DS 130 SEM and an EDAX 9600 quantitative energy dispersive X-ray analyzer were used to examine the electrode surface characteristics. X-ray diffraction analysis was carried out using a Rigaku X-ray diffractometer (model Dmax III-C) with Cu Kα radiation and a graphite monochromator.

Measurements were performed in solutions containing 0.05 M $ZnSO_4$ and different concentrations of AOT. In order to avoid the slow hydrolysis of AOT all the measurements were done with freshly prepared samples. All chemicals were reagent grade and solutions were made twice in distilled water.

Each set of experiments was repeated two to four times to ensure reproducibility.

3. Results and discussion

3.1. Voltammetric studies

Prior to the study of Zn deposition, the voltammetric response of the steel in 0.05 M Na_2SO_4 with and without AOT in the potential range between −0.5 V and −1.30 V was analyzed (Fig. 1). It can be seen that the curves are practically the same. This result indicates that the presence of AOT did neither affect the electrochemical response of the steel in the potential range analyzed nor the rate of the hydrogen evolution reaction.

For studying electrodeposition of Zn, the AOT concentration varied in the range 0.0–0.05 M while the $ZnSO_4$ concentration was kept constant at 0.05 M. The potential at which Zn^{2+} reduction starts is shifted to negative values by the addition of AOT. The onset of the reaction was observed at −1.040 V for 0.05 M $ZnSO_4$ and −1.090 V after addition of 0.05 M AOT. Furthermore with the increase in the surfactant content to 0.05 M, the total charge recorded at more negative potentials diminishes (Fig. 2). On the other hand, addition of AOT also affects the anodic process following electrodeposition. When AOT is added two anodic peaks (A and B) can be clearly distinguished, being higher the relative contribution of the peak (B).

The anodic response also depends on the negative limit of the scan range. Fig. 3 shows the cyclic voltammograms obtained at different switching potentials. If the potential scan is reversed at −1.14 V only a small anodic peak (peak A) is observed but when the negative scan is extended to −1.15 V, a new oxidation peak (peak B) appears at more positive potentials. Both peak heights increase upon extending the negative limit potential but the increase in the height of peak B is more noticeable.

The effect of the potential scan rate on the voltammetric response is shown in Fig. 4A. A linear relationship between the cathodic peak current density and the square root of scan rate is obtained (Fig. 4B), indicating that the cathodic process is controlled by mass transfer [13]. Considering that the intercept is greater than zero an additional process other than diffusion occurs [14]. The current density of the anodic peak (A) is practically independent of the scan rate while that corresponding to peak (B) varies with the square root of scan rate (Fig. 4C).

The measured cathodic currents increase under electrode rotation conditions (Fig. 5) On the other hand, the two well-defined anodic peaks are not observed in this case.The formation of a low amount of a flocculated material in the electrodeposition solution was observed after several days of preparation. In order to investigate which compound is formed between Zn^{2+} and AOT, a 0.05 M AOT solution with a high concentration of the cation (0.5 M) was prepared. The whole solution turned cloudy, forming a white gelatinous material. This material was isolated by filtration and analyzed by inductively coupled plasma atomic emission spectrometry (ICP-AES). The analysis of the precipitate gave a Zn:S mole ratio of 2.6, indicating that the material is composed of a mixture of sodium (NaAOT) and zinc dioctylsulfosuccinate ($Zn(AOT)_2$). The occurrence of the latter compound is reported in the literature [15].

The presence of the surfactant in the electrodeposition solution causes changes on the voltammetric response. This result can be

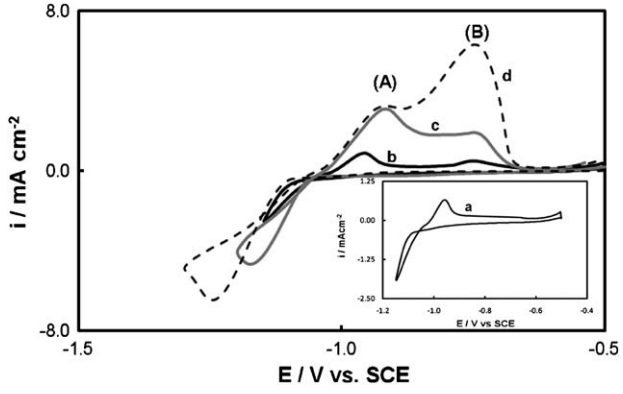

Fig. 3. Cyclic voltammograms for SAE 4140 steel electrode at 0.01 V s^{-1} in 0.05 M AOT + 0.05 M $ZnSO_4$, pH 6.3 solution, showing the effect of the negative scan limit: (a) −1.15 V, (b) −1.20 V, (c) −1.30 V and (d) −1.40 V. Initial potential: −0.50 V. The first cycle is displayed. The temperature was 20 °C.

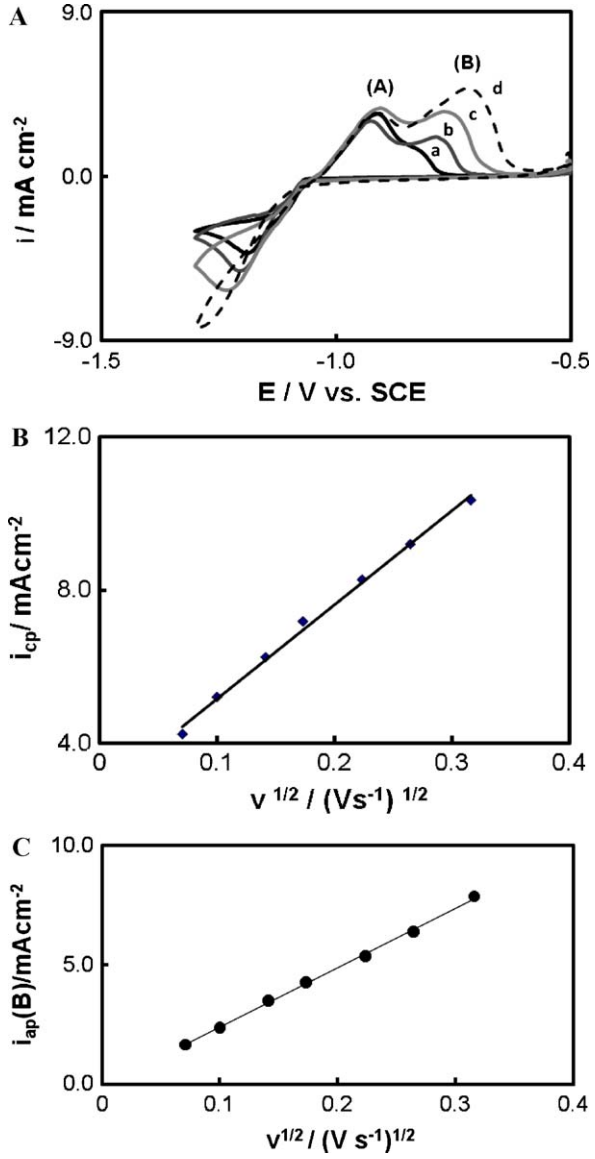

Fig. 4. (A) Cyclic voltammograms for SAE 4140 steel electrode in 0.05 M AOT + 0.05 M $ZnSO_4$, pH 6.3 solution obtained at: (a) 0.005 V s^{-1}, (b) 0.01 V s^{-1} (c) 0.02 V s^{-1} and (d) 0.05 V s^{-1}. Initial potential: −0.50 V. The first cycle is displayed. (B) Variation of cathodic peak current density with the square root of scan rate. (C) Variation of anodic peak current density (peak B) with the square root of scan rate. The temperature was 20 °C.

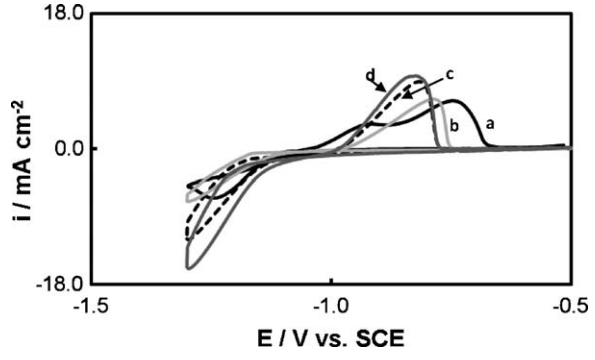

Fig. 5. Cyclic voltammograms for SAE 4140 steel electrode in 0.05 M AOT + 0.05 M $ZnSO_4$, pH 6.3 solution, at: (a) w = 0 rpm, (b) w = 800 rpm, (c) w = 1500 rpm and (d) 3000 rpm. Initial potential: −0.50 V. Scan rate: 0.05 V s^{-1}. The first cycle is displayed. The temperature was 20 °C.

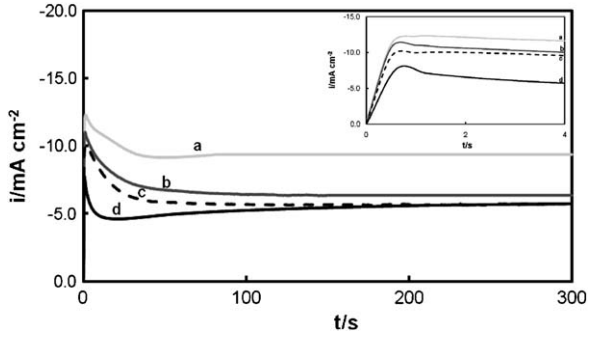

Fig. 6. Potentiostatic transients obtained for a SAE 4140 steel electrode at −1.30 V for 300 s in 0.05 M ZnSO4 + x M AOT, pH 6.3 solution with: (a) x = 0, (b) x = 0.005, (c) x = 0.01 and (d) x = 0.05. The electrodeposition temperature was set at 20 °C.

explained considering that surfactant adsorption provokes a blockage of the active sites available for Zn^{2+} discharge. It is known that at the cmc the non-aggregate state of surfactants changes to the aggregate dispersive state. The value of the cmc of AOT is 2.2 mM. Above the cmc, AOT molecules form micelles in the bulk solution and multiple layers at interfaces. It was reported that desorption of AOT from a Hg surface does not occur until a potential of −1.60 V is reached [16]. Thus, addition of the surfactant to the electrodeposition solution produces a decrease in the current associated with reduction of Zn^{2+} because the surface area for deposition decreases. The presence of AOT not only blocks active sites for deposition but also leads to the formation of $Zn(AOT)_2$, which should diffuse very slowly to the cathode.

The anodic curves obtained in the presence of the surfactant show two well-defined peaks (Figs. 3 and 4). Sylla et al. considered that the appearance of this double peak is associated with what happens at more negative potentials, where the hydrogen evolution is more intense [17]. Water reduction reaction and hydrogen evolution increase the interfacial pH, causing the formation of $Zn(OH)_2$ at more negative potentials. The presence of $Zn(OH)_2$ film covering part of the Zn electrodeposits reduces the dissolution rate of the metal and the corresponding oxidation reaction takes place at more positive potentials. This hypothesis is supported by the fact that the relative contribution of the peak at the more positive potentials (peak B) increases when: (i) the scan is extended to a more negative limit potential; (ii) the scan rate decreases and (iii) the electrode is rotated. Thus, it seems that the surfactant promotes the formation of $Zn(OH)_2$.

3.2. *I–t transients*

Fig. 6 shows the *I–t* transients obtained at −1.30 V for different AOT concentrations. The current density decreases as the AOT concentration increases, in accordance with the voltammetric results. The curves show the typical shape for a nucleation process. An initial current peak is seen (see inset in Fig. 6). Also, measurements were repeated several times to verify the reproducibility of the transient. At the end of the experiment, a thick and adherent deposit was formed that could only be removed on mechanical polishing. According to the standard cellotape test, the adherence was found to be independent of the deposition time.

The maximum current density (I_m) and the time required to reach it (t_m) increase when the applied potential is more negative (not shown here).

The relationship of dimensionless I/I_m versus t/t_m (where I_m and t_m are the current transient maximum values) obtained from the initial stages of electrodeposition is compared to the theoretical values corresponding for 3D instantaneous and progressive nucleation with diffusion-controlled growth [18] (Fig. 7). It can be seen

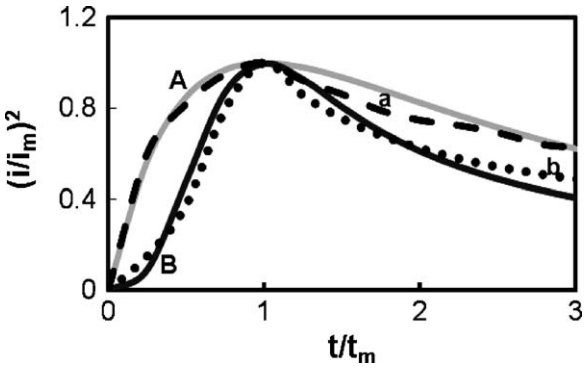

Fig. 7. Comparison of the dimensionless experimental current–time transients obtained for a SAE 4140 steel electrode in: (a) 0.05 M $ZnSO_4$ and (b) 0.05 M $ZnSO_4$ + 0.05 M AOT, pH 6.3 solution with the theoretical curves for three-dimensional instantaneous (curve A) and progressive nucleation (curve B). The electrodeposition temperature was set at 20 °C.

that the experimental data for deposition in the surfactant-free solution follow the curve for 3D instantaneous nucleation model, while those obtained in 0.05 M AOT solution agree well with the model for 3D progressive nucleation. The current density increases again at the longer times in the presence of the surfactant, probably due to an increased area for deposition.

As was expected, the blocking layer has an important effect on the nucleation and growth of the deposits due to the bulky structure of the branched tails of the AOT molecule.

The chronoamperometric response using vitreous carbon as a substrate is qualitatively similar to that obtained for the steel electrode, except that the current densities are higher and that the maximum appears at a longer time.

3.3. X-ray diffraction study

Fig. 8 shows the diffractograms obtained for samples prepared with and without AOT by employing the same electrodeposition charge. In both cases the deposits are formed by Zn. The diffraction lines for the electrodeposits formed in the solution without AOT are more intense (Fig. 8A), indicating the presence of a more crystalline structure. The relative intensity of the lines indicates a strong ⟨1 0 1⟩ orientation of the Zn coating.

3.4. Morphology

The deposits obtained from a solution without AOT at a fixed potential of −1.30 V are constituted by platelets with dimensions in the order of 0.5 μm having a vertical alignment (Fig. 9) in accordance with other works [19]. The evolution of the morphology of the deposits obtained in the presence of the surfactant with time was followed by SEM (Fig. 10). After 20 s the surface of the working electrode was covered with a deposit with a labyrinthine structure (Fig. 10A). This morphology is very similar to that of Zn electrodeposits prepared from an ethylene glycol solution of zinc acetate [6]. A deposit with a high microporosity is also observed for a deposition time of 60 s (Fig. 10B). When the polarization time was increased a new growth over the earlier deposit starts and a film formed by porous agglomerates of particles with dimensions in the range of 0.5–1 μm, that tends to pile up can be observed (Fig. 10C and D). The microporous nature of Zn electrodeposits was confirmed by cyclic voltammetry studies in 0.05 M Na_2SO_4 (Fig. 11, curve a). It can be noticed that the current densities measured for the Zn-coated steel are significantly higher than those corresponding for a massive Zn electrode (Fig. 11, curve b). This result indicates the electroformation of a deposit with a high surface area.

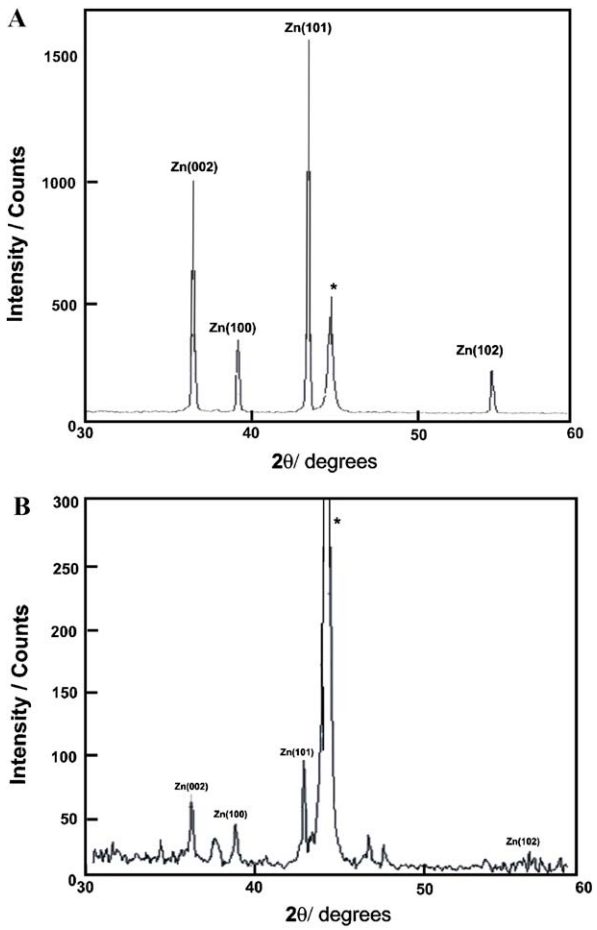

Fig. 8. X-ray diffraction pattern of Zn electrodeposits obtained at −1.30 V on SAE 4140 steel electrode in: (A) 0.05 M $ZnSO_4$ and (B). (A) 0.05 M $ZnSO_4$ + 0.05 M AOT, pH 6.3 solution. Diffraction lines due to the substrate (*). The electrodeposition temperature was set at 20 °C.

Fig. 12 shows the SEM images of Zn electrodeposits obtained on vitreous carbon. It can be seen that electrodeposits with a labyrinthine structure similar to that obtained on the steel surface under the same electrodeposition conditions (Fig. 10D). This fact indicates that the substrate type has not influenced the morphology of Zn electrodeposits.

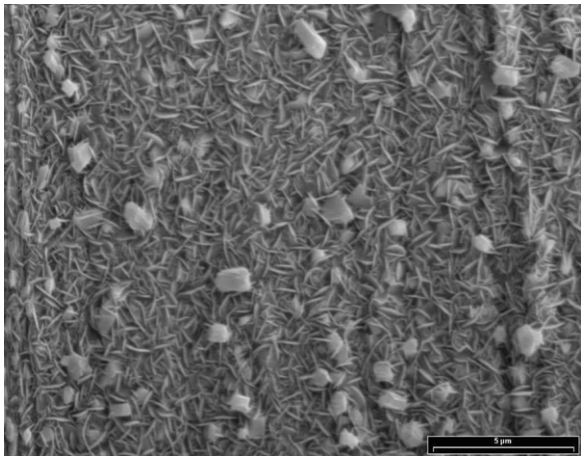

Fig. 9. SEM images of Zn electrodeposits obtained on SAE 4140 steel electrode at. −1.30 V for 60 s in 0.05 M $ZnSO_4$, pH 6.3 solution. The electrodeposition temperature was set at 20 °C.

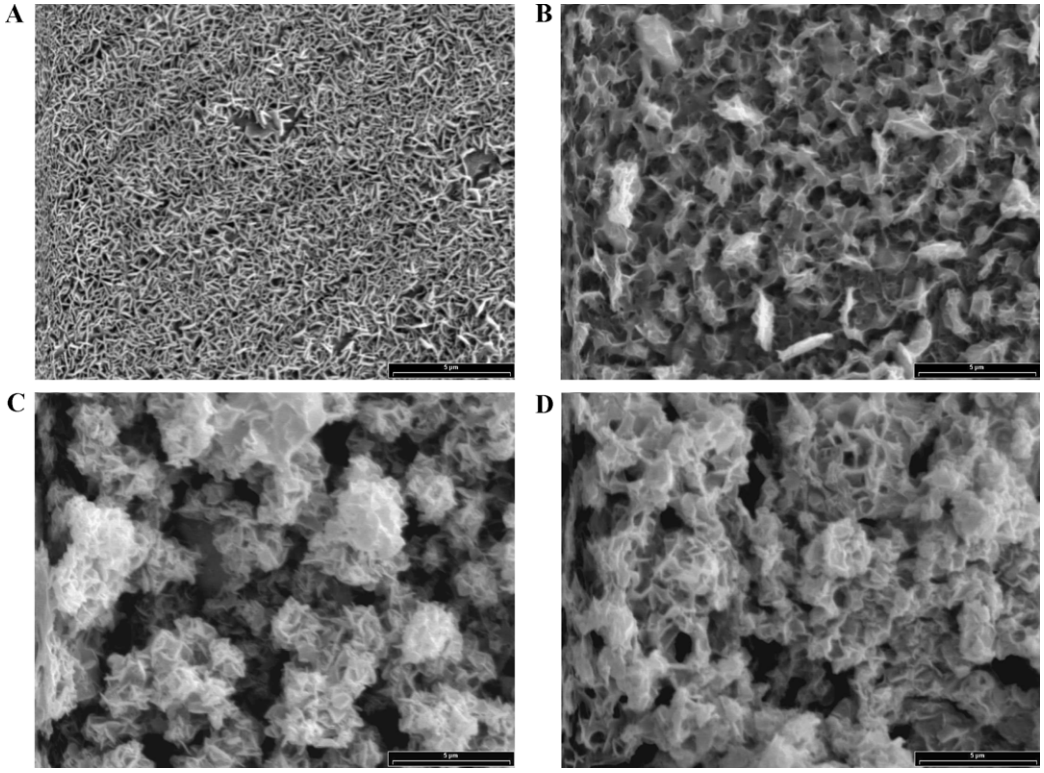

Fig. 10. SEM images of Zn electrodeposits obtained on SAE 4140 steel electrode at. −1.30 V in 0.05 M $ZnSO_4$ + 0.05 M AOT, pH 6.3 solution for: (A) 20 s, (B) 60 s,(C) 120 s, (D) 300 s. The electrodeposition temperature was set at 20 °C.

The effect of temperature on the morphology of electrodeposits can be observed in Fig. 13. When the electrodeposition temperature is 5 °C the morphology is similar to that obtained for 20 °C, but with less amount of agglomerates of particles (Fig. 13A). However, the number of agglomerates is higher when the temperature increases at 40 °C (Fig. 13B).

In order to remove any soluble material as, for example, $Zn(AOT)_2$, an electrode covered with Zn was immersed in water for 1 h. After this no major changes in morphology were observed. Furthermore, the EDX spectrum of Zn electrodeposits obtained from a solution containing AOT presents a weak signal of S. These results indicate that no significant amount of AOT is incorporated in the deposit (Fig. 14). According to other works, the oxygen signal can be explained by the presence of $Zn(OH)_2$ [20].

As was stated above, AOT blocks the active sites for deposition and leads to the formation of $Zn(AOT)_2$. On the other hand, AOT can be also adsorbed on the freshly deposited Zn making difficult the growth of nuclei as well as further deposition of new nuclei. All these facts lead to the formation of a three-dimensional net of deposited Zn instead of a continuous film. This final morphology is independent of the substrate characteristics. Thus, electrodeposition in the presence of AOT seems to be an optimal condition for incorporating metallic Zn in different matrices such as the modification of conducting polymers. In these cases the objective is to maximize the contact area between the metal and the matrix.

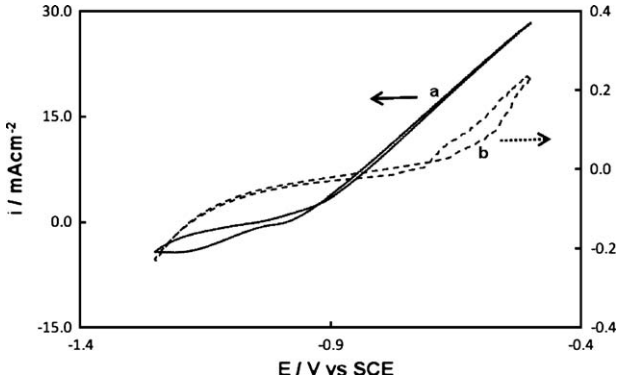

Fig. 11. Cyclic voltammograms at 0.05 V s^{-1} in 0.05 M Na_2SO_4 for: (a) Zn-coated SAE 4140 steel and (b) Zn electrode. The electrodeposits were obtained at −1.30 V in 0.05 M $ZnSO_4$ + 0.05 M AOT, pH 6.3 solution. Initial potential: −0.5 V. The first cycle is displayed. The temperature employed was 20 °C.

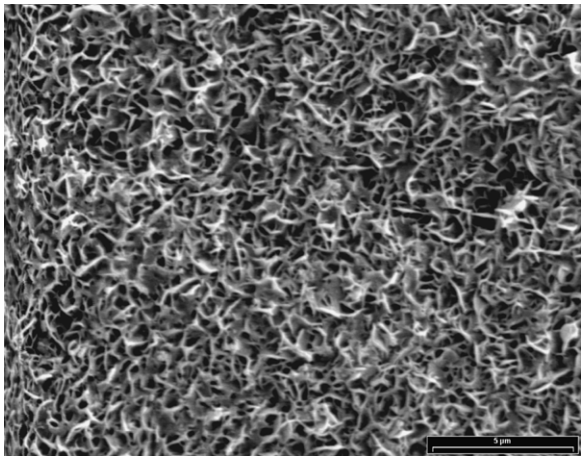

Fig. 12. SEM images of Zn electrodeposits obtained on vitreous carbon electrode at −1.30 V for 60 s in 0.05 M $ZnSO_4$ + 0.05 M AOT, pH 6.3 solution. The electrodeposition temperature was set at 20 °C.

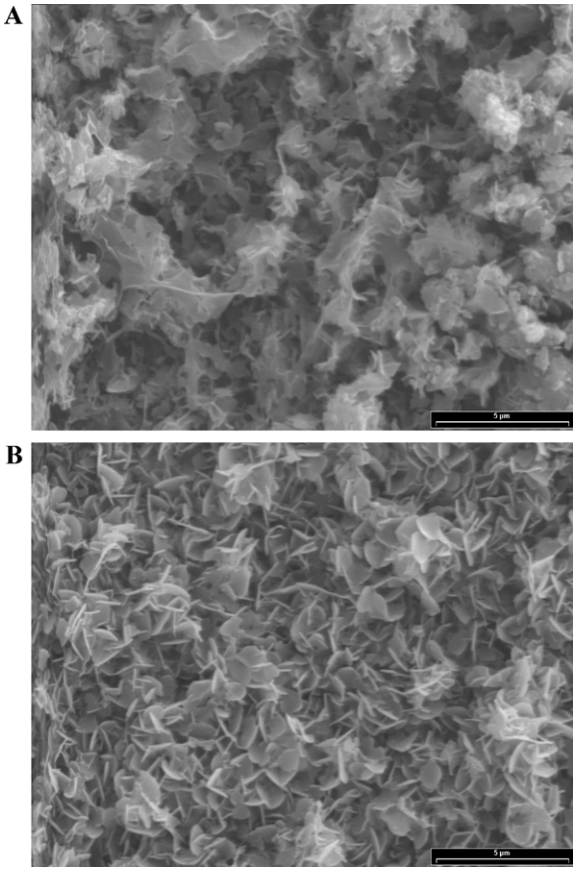

Fig. 13. SEM images of Zn electrodeposits formed on SAE 4140 steel electrode at −1.30 V in 0.05 M $ZnSO_4$ + 0.05 M AOT, pH 6.3 solution at: (A) 5 °C and (B) 40 °C. For both cases, the electrodeposition charge was the same as that consumed at 20 °C during 300 s.

3.5. Response of Zn-coated steel electrodes in chloride media

The polarization behavior in 0.5 M NaCl solution of the SAE 4140 steel electrode covered by Zn is presented in Fig. 15, curve b. The curve shows a current peak corresponding to the oxidation of Zn electrodeposits which initiates at −1.01 V. At more positive potentials an increase in the current density is observed for the sample at a potential value close to the corrosion potential of the uncoated steel (Fig. 15, curve a).

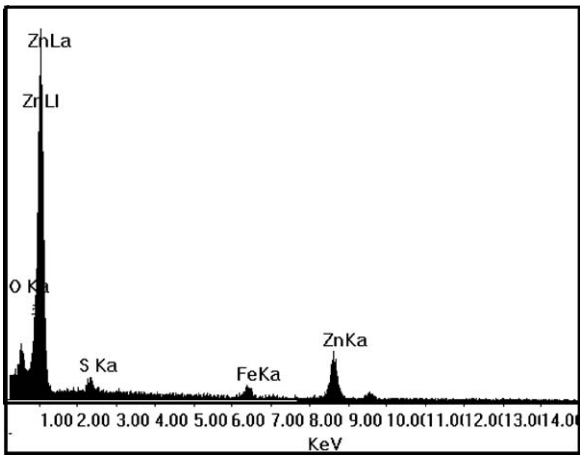

Fig. 14. EDX Spectrum of Zn electrodeposits obtained at −1.30 V on SAE 4140 steel electrode in 0.05 M $ZnSO_4$ + 0.05 M AOT, pH 6.3 solution. The sample was immersed in water for 1 h after removal from the solution. The electrodeposition temperature was set at 20 °C.

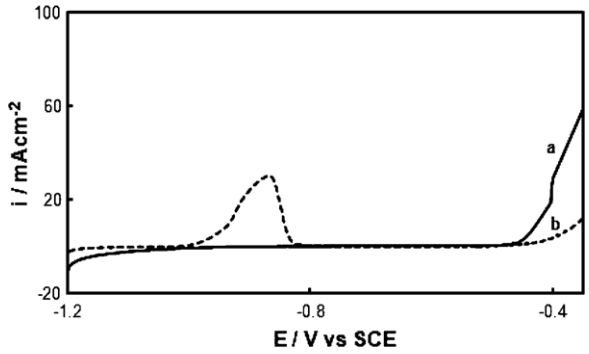

Fig. 15. The polarization behavior in 0.5 M NaCl at 0.0005 V s^{-1} of: (a) SAE 4140 steel electrode and (b) Zn-coated SAE 4140 steel electrode. The metallic deposits were electroformed at −1.30 V for 600 s in 0.05 M $ZnSO_4$ + 0.05 M AOT, pH 6.3 solution. The electrodeposition temperature was set at 20 °C.

A steel sample covered with a Zn deposit formed at −1.30 V in 0.05 M AOT + 0.05 M $ZnSO_4$, pH 6.3 solution during 600 s was immersed in 0.5 M NaCl solution as corrosive medium. Fig. 16 presents the evolution of OCP with the immersion time. Initially the OCP was about −1.08 V and corresponds to the corrosion potential of Zn. The OCP gradually shifts to more positive potentials until reaching the value corresponding to the steel over the course of an hour.

It is well known that a Zn coating can provide either barrier or galvanic protection to a steel substrate. The above mentioned results indicate that the Zn coating does not provide an efficient barrier against corrosion. The low corrosion resistance of the sample is explained considering the very porous structure of the deposit that allows chloride ions reaching the steel surface after a short period of immersion.

The Nyquist plots recorded at OCP for the Zn-coated steel electrode are presented in Fig. 17, curves a and b. For comparative purposes, the impedance response of the uncoated steel electrode is also presented (Fig. 17, curve c). At the beginning of immersion the diagram for the coated steel is very different to that obtained for bare steel. It shows a high-frequency depressed semicircle and at lower frequencies a linear part, which is probably associated with the diffusion of electrolyte through the porous Zn film. As the exposure time increases, the diagram tends to approach the curve of the uncoated steel. This is probably related to the poor anticorrosive performance of the Zn coating.

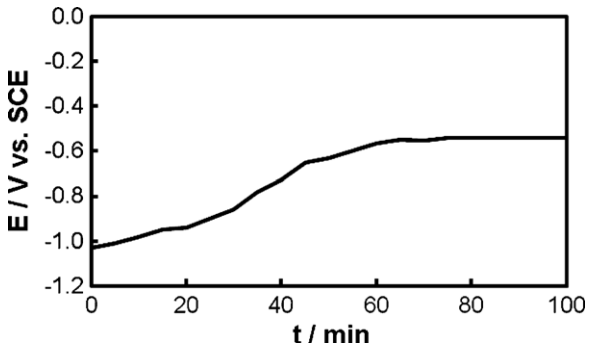

Fig. 16. Time dependence of the OCP in 0.5 M NaCl of Zn-coated SAE 4140 steel electrode. The metallic deposits were electroformed at −1.30 V for 600 s in 0.05 M $ZnSO_4$ + 0.05 M AOT, pH 6.3 solution. The electrodeposition temperature was set at 20 °C.

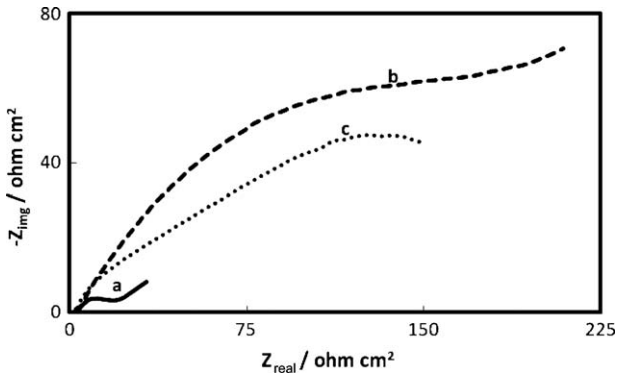

Fig. 17. Nyquist plots of the impedance spectrum in 0.5 M NaCl at the open circuit potential for: (a) Zn-coated SAE 4140 steel at the first stages of immersion, (b) Zn-coated SAE 4140 steel, immersion time: 45 min; and (c) SAE 4140 steel, immersion time: 45 min. The metallic deposits were electroformed at −1.30 V for 600 s in 0.05 M ZnSO4 + 0.05 M AOT, pH 6.3 solution. The electrodeposition temperature was set at 20 °C.

4. Conclusions

The presence of AOT in the electrolyte solution causes significant changes on the electrodeposition process. X-ray diffraction and EDX measurements showed the presence of Zn as the main element on the deposits obtained in AOT-containing solution. Parts of the deposits should be covered by $Zn(OH)_2$.Surface blocking by adsorbed surfactant and the presence of $Zn(AOT)_2$ alter the nucleation and growth stages leading to the formation of a porous coating. The morphology of the deposits change with time during a potentiostatic polarization, but always a high microporosity is observed. The described procedure is a promising approach to achieve adherent Zn films with a large surface area.

Acknowledgements

CONICET, ANPCYT and Universidad Nacional del Sur, Bahía Blanca, Argentina are acknowledged for financial support.

References

[1] R. Vittal, H. Gomathi, K.J. Kim, Beneficial role of surfactants in electrochemistry and in the modification of electrodes, Adv. Colloid Interface Sci. 119 (2006) 55–68.
[2] U. Retter, M. Tchachnikova, On the formation of surface micelles at the metal electrolyte interface, J. Electroanal. Chem. 550/551 (2003) 201–208.
[3] T. Tüken, B. Yazici, M. Erbil, Zinc modified polyaniline coating for mild steel protection, Mater. Chem. Phys. 99 (2006) 459–464.
[4] P. Herrasti, F.J. Recio, P. Ocón, E. Fatás, Effect of the polymer layers and bilayers on the corrosion behaviour of mild steel: comparison with polymers containing Zn microparticles, Prog. Org. Coat. 54 (2005) 285–291.
[5] A. Pepe, M. Aparicio, S. Ceré, A. Durán, Synthesis of hybrid silica sol–gel coatings containing Zn particles on carbon steel and Al/Zn coated carbon steel, Mater. Lett. 59 (2005) 3937–3940.
[6] G. Zou, W. Chen, R. Liu, Z. Xu, Orientation enhancement of polycrystalline ZnO thin films through thermal oxidation of electrodeposited zinc metal, Mater. Lett. 61 (2007) 4305–4308.
[7] H.B. Muralidhara, Y. Arthoba Naik, Electrochemical deposition of nanocrystalline zinc on steel substrate from acid zincate bath, Surf. Coat. Technol. 202 (2008) 3403–3412.
[8] S. Sungkaew, C. Thammakhet, P. Thavarungkul, P. Kanatharana, A new polyethylene glycol fiber prepared by coating porous zinc electrodeposited onto silver for solid-phase microextraction of styrene, Anal. Chim. Acta 664 (2010) 49–55.
[9] Y. Jun Chen, B. Chi, H. Zhou Zhang, H. Chen, Y. Chen, Controlled growth of zinc nanowires, Mater. Lett. 61 (2007) 144–147.
[10] I.L. Lehr, S.B. Saidman, Electrodeposition of polypyrrole on aluminium in the presence of sodium bis(2-ethylhexyl) sulfosuccinate, Mater. Chem. Phys. 10 (2006) 262–267.
[11] I.L. Lehr, S.B. Saidman, Corrosion protection of iron by polypyrrole coatings electrosynthesised from a surfactant solution, Corros. Sci. 49 (2007) 2210–2225.
[12] D.O. Flamini, S.B. Saidman, Characterization of polypyrrole films electrosynthesized onto titanium in the presence of sodium bis(2-ethylhexyl) sulfosuccinate (AOT), Electrochim. Acta 55 (2010) 3727–3733.
[13] A.J. Bard, L.R. Faulkner, Electrochemical Methods: Fundamental and Applications, 1st ed., J. Wiley & Sons, New York, 1980.
[14] G. Trejo, R. Ortega, Y. Meas, V.P. Ozil, E. Chainet, B. Nguyen, Nucleation and growth of zinc from chloride concentrated solutions, J. Electrochem. Soc. 145 (1998) 4090–4097.
[15] J. Eastoe, G. Fragneto, B.H. Robinson, T.F. Towey, R.K. Heenan, F.J. Leng, Variation of surfactant counterion and its effect on the structure and properties of aerosol-OT based water-in-oil microemulsions, J. Chem. Soc. Faraday Trans. 88 (1992) 461–471.
[16] A. Avranas, N. Papadopoulos, S. Sotiropoulos, Adsorption behavior of bis(2-ethylhexyl) sodium sulfosuccinate (AOT) at the mercury-electrolyte solution interface as a function of electrode potential and time, Prog. Colloid Polym. Sci. 272 (1994) 1252–1258.
[17] D. Sylla, C. Savall, M. Gadouleau, C. Rebere, J. Creus, Ph. Refait, Electrodeposition of Zn–Mn alloys on steel using an alkaline pyrophosphate-based electrolytic bath, Surf. Coat. Technol. 200 (2005) 2137–2145.
[18] B. Scharifker, G. Hills, Theoretical and experimental studies of multiple nucleation, Electrochim. Acta 28 (1983) 879–889.
[19] G. Trejo, H. Ruiz, R. Ortega Borges, Y. Meas, Influence of polyethoxylated additives on zinc electrodeposition from acidic solutions, J. Appl. Electrochem. 31 (2001) 685–692.
[20] A. Gomes, M.I. da Silva Pereira, Pulsed electrodeposition of Zn in the presence of surfactants, Electrochim. Acta 51 (2006) 1342–1350.